

JAAS

Accepted Manuscript



This is an *Accepted Manuscript*, which has been through the Royal Society of Chemistry peer review process and has been accepted for publication.

Accepted Manuscripts are published online shortly after acceptance, before technical editing, formatting and proof reading. Using this free service, authors can make their results available to the community, in citable form, before we publish the edited article. We will replace this *Accepted Manuscript* with the edited and formatted *Advance Article* as soon as it is available.

You can find more information about *Accepted Manuscripts* in the [Information for Authors](#).

Please note that technical editing may introduce minor changes to the text and/or graphics, which may alter content. The journal's standard [Terms & Conditions](#) and the [Ethical guidelines](#) still apply. In no event shall the Royal Society of Chemistry be held responsible for any errors or omissions in this *Accepted Manuscript* or any consequences arising from the use of any information it contains.

1
2
3
4
5 **1 Effects of Mercury and Thallium Concentrations on High Precision Determination of**
6
7
8 **2 Mercury Isotope Composition by Neptune Plus Multiple Collector Inductively Coupled**
9
10
11 **3 Plasma Mass Spectrometry**
12
13
14
15
16

17 Runsheng Yin^{a, b, *}, David P. Krabbenhoft^c, Bridget A. Bergquist^d, Wang Zheng^e, Ryan F.
18 Lepak^b, James P. Hurley^{b, f, *}
19
20
21

22
23 ^aState Key Laboratory of Ore Deposit Geochemistry, Institute of Geochemistry, Chinese
24 Academy of Sciences, Guiyang 550002, China
25

26 ^bEnvironmental Chemistry and Technology Program, University of Wisconsin-Madison,
27 Madison, WI, 53706, USA
28
29

30 ^cU.S. Geological Survey, Mercury Research Laboratory, Middleton, WI, 53562, USA
31

32 ^dUniversity of Toronto, Department of Earth Sciences, 22 Russell Street, Toronto, Ontario
33 M5S 3B1, Canada
34

35 ^eArizona State University, School of Earth and Space Exploration, Tempe, AZ 85287, USA
36

37 ^fDepartment of Civil and Environmental Engineering, University of Wisconsin-Madison,
38 Madison, WI, 53706, USA
39
40

41
42

43 *contact author: Runsheng Yin (yinrunsheng2002@163.com) and James P. Hurley
44 (jphurley@wisc.edu)
45
46

47
48
49
50
51
52
53
54
55
56
57
58
59
60

Abstract

Thallium (Tl) has been widely used as an internal standard for mass bias correction during high precision mercury (Hg) isotope ratio measurements using multi-collector inductively coupled plasma mass spectrometry (MC-ICP-MS). However, a recent study by Georg and Newman¹ indicated the potential for Hg hydrides formation (HgH_x , $x=1, 2$) during Hg isotope measurements using the X skimmer cone with the Neptune Plus MC-ICP-MS. Mercury hydride formation could result in an artificial change in $^{205}\text{Tl}/^{203}\text{Tl}$. Due to this observation, the applicability of using Tl as an internal standard for instrumental mass bias correction during high precision Hg isotope measurements has been questioned. In this study, using an adapted gas/liquid phase separator for Hg introduction and NIST SRM 997 Tl standard for mass bias correction, mercury isotope measurements were performed by the Neptune Plus MC-ICP-MS. While we confirm Georg and Newman's¹ observations, we show that Hg hydride formation is less important when Hg isotope measurements are conducted with high Tl and low Hg concentrations. With careful sample-standard bracketing (with Hg concentration matching within 10%), we demonstrate that measuring 20 to 50 ng mL^{-1} of Tl and 0.5 to 3.0 ng mL^{-1} of Hg, high precision Hg isotope ratio measurements are achievable. We caution researchers using other Hg inlet systems to recognize the importance of Hg and Tl concentrations, and encourage optimization of these values during their Hg isotope measurements.

1. Introduction

Multi-collector inductively coupled plasma mass spectrometry (MC-ICP-MS) has enabled simultaneous determination of Hg's seven natural stable isotopes (196, 198, 199, 200, 201, 202 and 204)¹⁻⁹. Both mass dependent fractionation (MDF, reported as δ values) and mass independent fractionation (MIF, reported as Δ values) have been observed during a variety of chemical, physical, and biological processes. Large variations of $\delta^{202}\text{Hg}$ ($\sim 10\%$), $\Delta^{199}\text{Hg}$ ($\sim 10\%$) and $\Delta^{200}\text{Hg}$ ($\sim 1\%$) have been reported in environmental samples¹⁰⁻¹². Mercury

1
2
3
4 49 stable isotopes have been successfully used as tracers to understand the sources and fates of
5
6 50 Hg in the environment¹⁰⁻¹².

7
8
9 51 Mercury isotope measurements have been performed by two commercial MC-ICP-MS
10
11 52 systems, Nu-Plasma^{3, 7} and Thermo Finnigan Neptune^{1-2, 4-5, 8-9}. To enhance the ion sampling
12
13 53 efficiency and overall sensitivity, the new generation Neptune Plus MC-ICP-MS have
14
15 54 combined modified skimmer and sample cone geometries with enhanced interface pumping
16
17 55 configuration¹³. Compared to the H cone geometry, the X skimmer cone has been shown to
18
19 56 result in a seven-fold increase in sensitivity for Tl, and a 10-20% increase in sensitivity for
20
21 57 Hg¹. Thus, the sample quantity needed for isotope ratio measurements can be significantly
22
23 58 reduced. However, concern has been recently raised by the observation of Hg hydride
24
25 59 formation (HgH_x) when using the high-sensitivity X skimmer cones with a Neptune
26
27 60 MC-ICP-MS equipped with the Plus upgrade¹. Hg hydride formation has shown to result in
28
29 61 increased ²⁰³Tl beam intensities. Due to close isotopic mass to Hg, Tl has been widely used
30
31 62 as an internal standard for instrumental mass bias correction of Hg isotopes¹⁻⁹, using the
32
33 63 Russell equation to determine the instrumental mass bias factor (β):

$$34 \quad \beta = \ln[(^{205}\text{Tl}/^{203}\text{Tl}_{\text{true}})/(^{205}\text{Tl}/^{203}\text{Tl}_{\text{measured}})]/\ln(m^{205}/m^{203}) \quad (1)$$

35
36 64 where ²⁰⁵Tl/²⁰³Tl_{true} and ²⁰⁵Tl/²⁰³Tl_{measured} is the true (mass bias corrected) ratio (2.38714) and
37
38 65 the measured ratio of ²⁰⁵Tl/²⁰³Tl for NIST SRM 997 Tl standard, respectively; and m²⁰⁵ and
39
40 66 m²⁰³ are the masses of ²⁰⁵Tl and ²⁰³Tl, respectively. The estimated β is applied to the mass
41
42 67 bias correction of Hg isotopic ratios (equation 2):

$$43 \quad {}^{\text{xxx}}\text{Hg}/^{198}\text{Hg}_{\text{true}} = {}^{\text{xxx}}\text{Hg}/^{198}\text{Hg}_{\text{measured}} \times (m^{\text{xxx}}/m^{198})^{\beta} \quad (2)$$

44
45 68 where ^{xxx}Hg/¹⁹⁸Hg_{true} and ^{xxx}Hg/¹⁹⁸Hg_{measured} is the true and measured ratio of ^{xxx}Hg/¹⁹⁸Hg,
46
47 69 respectively; m^{xxx} and m¹⁹⁸ are the masses of ^{xxx}Hg and ¹⁹⁸Hg, respectively; and xxx are
48
49 70 199-204 amu. According to Georg and Newman¹, the increase of ²⁰³Tl beam intensity due to
50
51 71 Hg hydride formation could result in decreased ²⁰⁵Tl/²⁰³Tl_{measured}, which would unavoidably
52
53 72 cause artificial effect of the β (according to equation 1) and Hg isotope ratios (according to
54
55 73 equation 2). As a result, mercury hydride formation has raised significant concerns not only
56
57 74 to users of Neptune Plus MC-ICP-MS, but also to others using Tl for mass bias correction
58
59 75 for Hg isotope measurements¹.
60

1
2
3
4 78 In order to confirm whether the concerns of Hg hydride formation were directly
5
6 79 applicable to our analyses, we performed a series of independent tests based on well known
7
8 80 Hg standard solutions. It is worth noting that measurements by Georg and Newman¹ were
9
10 81 mainly based on high Hg concentrations (e.g., 5, 10 and 25 ng mL⁻¹). To our knowledge,
11
12 82 most Hg isotope data reported to date were mainly measured at low Hg concentrations (0.5
13
14 83 to 5 ng mL⁻¹)¹⁻⁹. Theoretically, effects of Hg hydride formation may be reduced by
15
16 84 measuring low Hg concentrations. To test this speculation, we performed Hg isotope
17
18 85 analysis at much lower Hg concentrations (0.3 to 3.0 ng mL⁻¹). We acknowledge the
19
20 86 potential for discrepancies between the Georg and Newman¹ and our own system due to
21
22 87 inlet system differences. The Cetac HGX-200 cold vapor system was used by Georg and
23
24 88 Newman¹ and others^{1-2, 4-5, 8-9}, however we used a adapted gas-liquid phase separator (Figure
25
26 89 1) which initially developed at University of Toronto, Department of Earth Sciences
27
28 90 laboratory. Our study, however, was designed to investigate the potential for artifact
29
30 91 formation using conditions typical of our laboratory's protocol for geological and
31
32 92 environmental samples.

33 93 **2. Experimental methods**

34 35 94 **2.1 Instrumentation and mercury isotope determination**

36
37 95 Mercury isotopic measurements were conducted on a Neptune Plus MC-ICP-MS housed at
38
39 96 the University of Wisconsin-Madison's State Laboratory of Hygiene. The instrument was
40
41 97 equipped with the gas-liquid phase separator (Figure 1) and an Apex-Q nebulizer (Elemental
42
43 98 Scientific Inc., USA) for Hg and Tl introduction, respectively. Briefly, stannous chloride
44
45 99 (SnCl₂) was continually pumped along with Hg(II) solutions and allowed to mix prior to
46
47 100 being introduced to a frosted glass phase separator, producing gaseous elemental Hg(0). The
48
49 101 Hg(0) was then mixed with the dry Tl aerosol generated by the Apex-Q nebulizer before
50
51 102 being introduced into the plasma. The Apex-Q nebulizer (free flow-mode) and the glass
52
53 103 phase separator were flushed with the "sample" gas (Ar) and "additional" gas (Ar) of the
54
55 104 MC-ICP-MS, respectively. NIST SRM 997 Tl standard (²⁰⁵Tl/²⁰³Tl = 2.38714) was used as
56
57 105 an internal standard for simultaneous instrumental mass bias correction of Hg. Seven of the
58
59 106 nine faraday cups were used to monitor the ¹⁹⁸Hg, ¹⁹⁹Hg, ²⁰⁰Hg, ²⁰¹Hg, ²⁰²Hg, ²⁰³Tl and ²⁰⁵Tl

1
2
3
4 107 isotopes, respectively (Table 1). The nickel X skimmer cone was combined with a jet cone.
5
6 108 Hg and Tl concentrations in solutions were monitored by ^{201}Hg and ^{203}Tl signals. The signals
7
8 109 for ^{201}Hg and ^{203}Tl were 0.6×10^{-2} and 0.2×10^{-2} V for acid blanks, respectively. Isobaric
9
10 110 interferences of ^{196}Pt , ^{198}Pt and ^{204}Pb were evaluated by measuring the peak intensities of
11
12 111 ^{194}Pt and ^{206}Pb , and no signals above background were observed ($< 10^{-4}$ V).

13
14 112 Gains of the amplifier associated with each Faraday collector were calibrated for
15
16 113 efficiency on a daily basis. Instrumental parameters (e.g., Ar gas flows, torch settings, and
17
18 114 lens system) were tuned for a maximum ion intensity of Hg and Tl in standard solutions
19
20 115 (Table 2). Data was acquired using 3 blocks each of 60 cycles, 2.097 seconds per cycle. An
21
22 116 initial uptake of sample solution for 3 min ensured stable signals before isotope analyses
23
24 117 were initiated. Between samples, the glass phase separator was rinsed using 3% (v/v) HNO_3
25
26 118 for 6 minutes until the signal intensity returned to background level. A sample-standard
27
28 119 bracketing (SSB) approach was used to compare relative per mil (‰) deviation (using the δ
29
30 120 notation) of all our measurements to NIST SRM 3133, according to Blum and Bergquist³:

31
32 121
$$\delta^{\text{xxx}}\text{Hg}(\text{‰}) = \left\{ \left(\frac{^{\text{xxx}}\text{Hg}/^{198}\text{Hg}_{\text{sample}}}{^{\text{xxx}}\text{Hg}/^{198}\text{Hg}_{\text{NIST SRM 3133}}} \right) - 1 \right\} \times 1000 \quad (3)$$

33
34 122 where xxx are 199, 200, 201 and 202 amu. Hg-MIF is reported in Δ notation ($\Delta^{\text{xxx}}\text{Hg}$,
35
36 123 deviation from mass dependency in units of permil, ‰) and is the difference between the
37
38 124 measured $\Delta^{\text{xxx}}\text{Hg}$ and the theoretically predicted $\Delta^{\text{xxx}}\text{Hg}$ value following equations by Blum
39
40 125 and Bergquist³:

41
42 126
$$\Delta^{199}\text{Hg} \approx \delta^{199}\text{Hg} - \delta^{202}\text{Hg} \times 0.2520 \quad (4)$$

43
44 127
$$\Delta^{200}\text{Hg} \approx \delta^{200}\text{Hg} - \delta^{202}\text{Hg} \times 0.5024 \quad (5)$$

45
46 128
$$\Delta^{201}\text{Hg} \approx \delta^{201}\text{Hg} - \delta^{202}\text{Hg} \times 0.7520 \quad (6)$$

47
48 129 **2.2 Reagents.**

49
50 130 SnCl_2 (3%, w/w) was prepared in 10% (v/v) HCl. In sections 2.3 and 2.4, all Hg solutions
51
52 131 were prepared by 3% HCl. We observed that using HCl is necessary to prevent the
53
54 132 volatilization of Hg from acidic solutions, whereas using 3% HNO_3 is insufficient. In section
55
56 133 2.5, acid mixtures (HCl, HNO_3 and H_2SO_4) were used to prepare the different standard
57
58 134 reference materials (SRMs). All acids used in this study were of ultrapure grades (certified
59
60 135 ACS Plus, Fisher Scientific), and 18.2 $\text{M}\Omega \cdot \text{cm}$ water (ELGA LabWater) was used for the
136 preparation of reagents and solutions.

1
2
3
4
5
6
7
8
9
10
11
12
13
14
15
16
17
18
19
20
21
22
23
24
25
26
27
28
29
30
31
32
33
34
35
36
37
38
39
40
41
42
43
44
45
46
47
48
49
50
51
52
53
54
55
56
57
58
59
60

137 **2.3 Measurements of varied Hg concentrations with consistent Tl concentrations.**

138 Four sequences were conducted to evaluate the effect of Hg concentration on Hg isotope
139 ratios. We prepared four different NIST SRM 997 standard solutions with variable Tl
140 concentrations (2, 20, 30 and 50 ng mL⁻¹). For each sequence, the concentration of Tl was
141 held constant, whereas we measured UM-Almadén secondary standard Hg solutions
142 containing 0.3, 0.5, 0.8, 1.2, 1.7, 2.3 to 3.0 ng mL⁻¹ of Hg. The bracketed NIST SRM 3133
143 Hg solutions were diluted to have same Hg concentrations of the UM-Almadén standard.
144 With the SSB approach, replicate measurements of UM-Almadén (n=4) and NIST SRM
145 3133 (n=5) of each specific Hg concentration were measured, which enabled measurement
146 reproducibility (n=4).

147 **2.4 Measurements of varied Tl concentrations with consistent Hg concentrations.**

148 Two sequences were performed to evaluate the effect of Tl concentrations on Hg isotope
149 ratios. We prepared two different NIST SRM 3133 Hg solutions with Hg concentrations of
150 0.5 and 1.0 ng mL⁻¹. The concentrations of NIST SRM 3133 was held constant during each
151 sequence, however, instrumental mass bias correction were performed by measuring NIST
152 SRM 997 with variable Tl concentrations (1, 2, 3, 4, 7, 15, 20, 30, 40, 50, 60, 100 ng mL⁻¹).
153 Replicate measurements (n=4) for a specific Tl concentration were conducted.

154 **2.4 Measurements of standard reference materials.**

155 For biological SRMs such as TORT-2 (Lobster), DORM-2 (Fish protein), DORM-3 (Fish
156 protein) and DOLT-2 (dogfish liver), about 0.2 g of each SRM was weighed and digested at
157 95 °C for 3 h with a 4 mL acid mixture (HNO₃:H₂SO₄= 7:3, v/v) following method by Pfeil
158 and Stalvey¹⁵. BrCl (200 µL) was later added to each sample and kept for 12 h to allow the
159 conversion of Hg to Hg(II). Hydroxylamine (400 µL) was added to the biological solutions
160 prior to Hg isotope measurements. For other SRMs such as NIST SRM 2711 (Montana Soil
161 II) and MESS-1 (marine sediment), about 0.2 g of ground sample was digested (95 °C, 1
162 hour) in a 2 mL aqua regia (HCl:HNO₃ = 3:1, v:v) according to Yin et al.¹⁶. For each SRM,
163 triplicate digests were prepared (n=3).

164 On basis of the certified total Hg concentrations for SRMs, about 5 and 10 ng Hg were
165 taken up and diluted to 0.5 and 1.0 ng mL⁻¹ of Hg, respectively. The acid solutions used for
166 dilution of biological SRMs were 10% HNO₃:H₂SO₄ mixture (7:3, v/v), whereas that used

1
2
3
4 167 for other SRMs are 10% HCl:HNO₃ (3:1, v/v). UM-Almadén and NIST SRM 3133 solutions
5
6 168 containing 0.5 and 1.0 ng mL⁻¹ of Hg were also prepared by 10% HNO₃:H₂SO₄ mixture (7:3,
7
8 169 v/v) and 10% HCl:HNO₃ (3:1, v/v) acid mixtures. During analysis, Hg concentrations and
9
10 170 acid matrices of the NIST SRM 3133 solutions were matched to the bracketed samples. THg
11
12 171 concentrations in the digest solutions were measured by the ²⁰¹Hg intensities, which showed
13
14 172 that the recoveries of Hg for the SRMs were 94 to 109%.

15 173 **2.5 Reporting uncertainties.**

16
17 174 For isotope ratios of Hg and Tl, uncertainties were reported using the theoretical statistical
18
19 175 errors (SE) of all cycles, which was automatically calculated by online data acquisition
20
21 176 software of the instrument. For δ and Δ values of UM-Almadén, uncertainties were reported
22
23 177 using the standard deviation (SD) of repeated measurements of the same solution; for δ and
24
25 178 Δ values of SRMs, uncertainties were reported using the SD values of the duplicate sample
26
27 179 digests.

28 29 180 **3. Results and discussion**

30 31 181 **3.1 Hg and Tl sensitivities during Hg isotope analysis.**

32
33 182 Sample uptake rates for Hg and Tl solutions in this study were about 0.65 and 0.05 mL min⁻¹,
34
35 183 respectively. Intensities of Hg and Tl showed linear correlations with Hg and Tl
36
37 184 concentrations as shown in Figure S1 of Supplemental Information (SI). The sensitivity of
38
39 185 ²⁰¹Hg (~0.56 V per ng mL⁻¹ Hg) of our study is higher than previous studies^{1-2, 4-5, 8-9}.
40
41 186 Sensitivity differences can be caused by a variety of factors, such as the type of cones and
42
43 187 the operating conditions of individual instrument, and the inlet system used for Hg
44
45 188 introduction^{1-2, 4-5, 8-9, 14, 17}.

46 47 189 **3.2 Effects of Hg and Tl concentrations on Tl isotope ratios.**

48
49 190 Our data confirm that varied Tl and Hg concentrations have a large effect on
50
51 191 ²⁰⁵Tl/²⁰³Tl_{measured} ratios (Figure 2A-C). When Tl concentration was held constant, increased
52
53 192 Hg concentration resulted in decreased ²⁰⁵Tl/²⁰³Tl_{measured} (Figure 2A). When measuring Hg
54
55 193 standards with similar Hg concentrations, the increase of Tl concentration resulted in
56
57 194 increased ²⁰⁵Tl/²⁰³Tl_{measured}, but such an increase was smaller at higher Tl concentration
58
59 195 (Figure 2B). The increase of ²⁰⁵Tl/²⁰³Tl_{measured} was small at higher Tl/Hg ratios (Figure 2C).

1
2
3
4 196 These results are consistent with the observation by Georg and Newman¹, which showed
5
6 197 that the formation of Hg hydride could result in increased ²⁰³Tl intensities and decreased
7
8 198 ²⁰⁵Tl/²⁰³Tl, when using Neptune Plus MC-ICP-MS with an X skimmer cone. By measuring
9
10 199 0.3 to 3.0 ng mL⁻¹ of Hg and without Tl introduction (only 3% HNO₃) by the Apex-Q, we
11
12 200 monitored the ²⁰³Tl and ²⁰⁵Tl intensities to evaluate the rate of Hg hydride formation. All our
13
14 201 measurements showed increased ²⁰³Tl intensities but no increase for ²⁰⁵Tl (Figure 3). This is
15
16 202 consistent with previous prediction that Hg hydride is mainly formed in HgH₂⁺ rather than
17
18 203 HgH⁺ species¹. A positive linear correlation was observed between ²⁰¹Hg and ²⁰³Tl
19
20 204 intensities, which indicated a rate of ~0.07% for HgH₂⁺ formation in our study (Figure 3)
21
22 205 and was comparable to that reported by Georg and Newman (0.1%)¹.

23
24 206 According to equation 1, artificial changes of ²⁰⁵Tl/²⁰³Tl_{measured} due to Hg hydride
25
26 207 formation should cause the shift of β values. Our results showed that when Tl concentrations
27
28 208 were held constant, increased Hg concentrations resulted in the increase of β (Figure 2D).
29
30 209 When measuring Hg standards with similar Hg concentrations, an increase in Tl
31
32 210 concentration caused negative shift of β, but the shift was small at high Tl concentration
33
34 211 (Figure 2E). For instance, measurements of high Tl solutions (20 to 50 ng mL⁻¹) resulted in
35
36 212 small shifts of <0.3 for β (Figure 2E), whereas measuring low Tl solutions (2 ng mL⁻¹)
37
38 213 resulted in a large shift of β of ~1 (Figure 2D). The shift of β was much smaller at high
39
40 214 Tl/Hg ratios (Figure 2F).

215 3.3 Effects of Hg and Tl concentrations to Hg isotopic ratios.

41 216 The mass-bias corrected ^{xxx}Hg/¹⁹⁸Hg_{true} ratios (e.g. ¹⁹⁹Hg/¹⁹⁸Hg_{true}, ²⁰⁰Hg/¹⁹⁸Hg_{true},
42
43 217 ²⁰¹Hg/¹⁹⁸Hg_{true} and ²⁰²Hg/¹⁹⁸Hg_{true}) are summarized in Table S1 (SI) and Figure 4. The mean
44
45 218 ratios for NIST SRM 3133 measurements (Table S1, SI) are in the range of previous results³,
46
47 219 ^{4, 9, 18}. The uncertainties of ^{xxx}Hg/¹⁹⁸Hg_{true} ratios are of the same magnitude with those
48
49 220 reported by Blum and Bergquist³, and Ridley and Stetson¹⁸, but smaller than those reported
50
51 221 by Berni et al.⁹. The larger uncertainties reported by Berni et al.⁹ are representative of a very
52
53 222 much longer period of time, accounting for variability within several measurement sessions
54
55 223 (480 measurements). Yang and Sturgeon⁴ also reported larger uncertainties of the
56
57 224 ^{xxx}Hg/¹⁹⁸Hg_{true} ratios, but their uncertainties were estimated as random error propagation, and
58
59 225 uncertainty from ²⁰⁵Tl/²⁰³Tl ratio was included in their reported Hg ratios. According to

1
2
3
4 226 equation 2, artificial shifts of β could unavoidably cause changes in mass-bias corrected Hg
5
6 227 isotope ratios. In our study, positive linear correlations between Hg concentrations and
7
8 228 $^{xxx}\text{Hg}/^{198}\text{Hg}_{\text{true}}$ ratios (e.g. $^{199}\text{Hg}/^{198}\text{Hg}_{\text{true}}$, $^{200}\text{Hg}/^{198}\text{Hg}_{\text{true}}$, $^{201}\text{Hg}/^{198}\text{Hg}_{\text{true}}$ and $^{202}\text{Hg}/^{198}\text{Hg}_{\text{true}}$)
9
10 229 were observed (Figure 4). When Tl concentration was constant, the rates of increase for
11
12 230 mass-bias corrected Hg isotope ratios were similar for UM-Almadén and NIST SRM 3133.
13
14 231 The slopes between $^{xxx}\text{Hg}/^{198}\text{Hg}_{\text{true}}$ and Hg concentrations were much higher at lower Tl
15
16 232 concentrations (Figure 4), consistent with the observation that lower Tl concentrations tend
17
18 233 to result in more artificial shift of β (Figures 2D and 2E). This observation confirms that
19
20 234 measuring lower Hg and higher Tl solution is necessary for Hg isotope measurements, and
21
22 235 that concentrations of Hg between samples and standards must be carefully matched, is
23
24 236 necessary for Hg isotope measurements.

237 **3.4 Optimization of Hg and Tl concentrations for Hg isotope measurement.**

238 Changes in Hg and Tl concentrations also affect the SE values of $^{xxx}\text{Hg}/^{198}\text{Hg}_{\text{true}}$ ratios
239 (Figure 5). Using low Tl standard of 2 ng mL⁻¹, the SE of $^{xxx}\text{Hg}/^{198}\text{Hg}_{\text{true}}$ ratios is much higher
240 than high Tl standards (20, 30, and 50 ng mL⁻¹). The high SE of $^{xxx}\text{Hg}/^{198}\text{Hg}_{\text{true}}$ ratios using
241 low Tl standard (2 ng mL⁻¹) could be explained by the fact that the precision of
242 $^{205}\text{Tl}/^{203}\text{Tl}_{\text{measured}}$ is compromised at lower Tl concentrations (Figure 6B). Using higher Tl
243 standards (20, 30, and 50 ng mL⁻¹), the SE of $^{xxx}\text{Hg}/^{198}\text{Hg}_{\text{true}}$ ratios decreased as Hg
244 concentration increased (Figure 5), similar to previous observations by Foucher and
245 Hintelmann². The SE of $^{202}\text{Hg}/^{198}\text{Hg}_{\text{true}}$ decreased from 0.00008 to 0.00004 as Hg
246 concentrations increased from 0.3 to 3.0 ng mL⁻¹, which is only equivalent 0.02‰ to 0.03‰
247 changes for $\delta^{202}\text{Hg}$. No significant decreases of the SE for $^{xxx}\text{Hg}/^{198}\text{Hg}_{\text{true}}$ were observed
248 when Hg concentrations were above 0.5 ng mL⁻¹, whereas increasing Hg concentrations
249 would (1) increase the rinsing time and the risk of carry over between samples; and (2)
250 increase the sample quantities for measurements. We suggest that Hg concentrations of 0.5
251 to 1.0 ng mL⁻¹ should be the best compromise between obtainable precision, rinsing time and
252 analyte consumption.

253 Varied Tl concentrations (1, 2, 3, 4, 7, 15, 20, 30, 40, 50, 60, 100 ng mL⁻¹) were
254 measured to evaluate the optimum concentrations of Tl when measurements were performed
255 at specific Hg concentrations of 0.5 and 1.0 ng mL⁻¹. We observed that the $^{205}\text{Tl}/^{203}\text{Tl}_{\text{measured}}$

1
2
3
4 256 increased exponentially with the increase of Tl concentrations, whereas the SE of
5 257 $^{205}\text{Tl}/^{203}\text{Tl}_{\text{measured}}$ and β decreased (Figure 6). As shown in Figure S2, the SE of $^{xxx}\text{Hg}/^{198}\text{Hg}_{\text{true}}$
6
7 258 is positive correlated with the SE of $^{205}\text{Tl}/^{203}\text{Tl}_{\text{measured}}$. Hg isotope ratios and their SE values
8
9 259 decreased significantly with the increase of Tl concentrations until the Tl concentrations
10
11 260 were beyond 20 ng mL⁻¹ (Figure 7). For our instrument therefore, we suggest at least 20 ng
12
13 261 mL⁻¹ of Tl should be used during high precision Hg isotope measurement.

262 **3.5 Importance to match Hg concentrations between Hg solutions and NIST SRM**

263 **3133.**

18 264 The SSB approach is a common practice to correct for mass bias of Hg isotope measurement
19
20 265 with the assumption that samples and bracketing standards are subjected to similar mass
21
22 266 bias³. However, our results showed that mass bias is in fact, concentration dependent (Figure
23
24 267 4), so the SSB requires concentration match between sample and standard. We evaluated the
25
26 268 effect of mismatch in Hg concentrations between UM-Almadén and NIST SRM 3133
27
28 269 [termed as $\text{THg}_{\text{UM-Almadén}}/\text{THg}_{\text{NIST SRM 3133}} - 1$ (%)] on Hg isotopic compositions. Mean Hg
29
30 270 isotope ratios of UM-Almadén and NIST SRM 3133 with the same Hg concentrations were
31
32 271 calculated, then mean Hg isotope ratio of UM-Almadén with a certain Hg concentration
33
34 272 were bracketed by that of NIST SRM 3133 with other Hg concentrations. As shown in
35
36 273 Figure 8, the isotopic composition of Hg for concentrations matched within 10% agreed with
37
38 274 published values³, whereas the THg mismatched results show large deviations in both $\delta^{202}\text{Hg}$
39
40 275 values and Δ values (Figure 8). It appears as though bracketing with higher NIST SRM 3133
41
42 276 concentration results in more negative $\delta^{202}\text{Hg}$, whereas bracketing with lower NIST SRM
43
44 277 3133 concentration results in $\delta^{202}\text{Hg}$ that is larger than the reported number. This can be
45
46 278 explained by positive linear correlations between Hg concentrations and measured
47
48 279 $^{202}\text{Hg}/^{198}\text{Hg}$ (Figure 4). The calculated values for UM-Almadén (Figure 8) highlight the
49
50 280 importance of concentration matching while using the SSB method.

51
52 281 The δ and Δ values of UM-Almadén, based on Hg concentration matched NIST SRM
53
54 282 3133, were estimated (Table S2, SI). With the exception of the analysis using a 2 ng mL⁻¹ Tl
55
56 283 internal standard, all analysis showed consistent δ and Δ values that is in well agreement
57
58 284 with previous results³. Our results suggest that high precision measurements of Hg isotopes
59
60 285 should be performed based on higher Tl internal standards. Typically, for low Hg solutions

1
2
3 286 (0.3 to 3.0 ng mL⁻¹) measured in our study, results of δ and Δ values were consistent for
4
5 287 internal standards containing ≥ 20 ng mL⁻¹ of Tl. Theoretically, accurate Hg isotope
6
7 288 measurements for high Hg solutions may be also achieved by increasing the concentrations
8
9 289 of Tl for mass bias correction. However, this is not necessary considering that higher Hg and
10
11 290 Tl concentrations will result in larger rinsing time and analyte consumption. In previous
12
13 291 studies from our laboratory, most measurements are based on 0.5 to 1 ng mL⁻¹ Hg and 20 ng
14
15 292 mL⁻¹ Tl solutions. A minimum of at least 4 to 8 ng of Hg per measurement (an initial uptake
16
17 293 of 3 min for signal stabilization plus ~ 7 min of acquisition, sample solution uptake: 0.65 mL
18
19 294 min⁻¹) is required to reach precise determination of $\delta^{202}\text{Hg}$ (within $\pm 0.10\%$, 2sd).

20 295 **3.6 Mercury isotope composition of standard reference materials.**

21
22 296 As mentioned in Section 2.5, SRMs were measured to test the potential isotope bias during
23
24 297 measurements of different environmental matrices. All tests were performed with low Hg
25
26 298 solutions containing 0.5 and 1.0 ng mL⁻¹ of Hg, and high internal standard containing 20 ng
27
28 299 mL⁻¹ of Tl. Based on well-matched THg concentrations and acid matrices between samples
29
30 300 and the bracketed NIST SRM 3133, the measured Hg isotope composition and uncertainties
31
32 301 for SRMs (Table S3, SI) were in agreement with previous studies^{6, 16, 19-22}.

33 302 **4. Conclusion**

34
35
36
37 303 While our study agrees with the results by Georg and Newman¹, that measuring Hg isotopes
38
39 304 by Neptune Plus MC-ICP-MS with high sensitivity X skimmer cones may result in
40
41 305 interference to $^{205}\text{Tl}/^{203}\text{Tl}$ ratio and inaccurate mass bias determination due to Hg hydride
42
43 306 formation. We confirm these interferences can be minimized when higher Tl (20 to 50 ng
44
45 307 mL⁻¹) and lower Hg (0.5 to 3 ng mL⁻¹) concentrations are introduced. Based on careful
46
47 308 optimization of Tl and Hg concentrations, combined with carefully matched Hg
48
49 309 concentration between samples and bracketing standards, we demonstrated that accurate Hg
50
51 310 isotopic measurements can be achieved. We acknowledge that our measurements were
52
53 311 performed using an adapted inlet system, which may not directly apply to other introduction
54
55 312 systems such as the Cetac HGX-200. Therefore, we advise other Neptune users perform
56
57 313 internal optimization steps to minimize potential for matrix effects when measuring Hg
58
59 314 isotopes.

1
2
3
4 315 **Acknowledgments.** We thank Joel D. Blum (University of Michigan) for providing
5 316 UM-Almadén standard solution, and strengthening this manuscript. This work was
6
7 317 supported by the Natural Science Foundation of China (No: 41303014). Four anonymous
8
9 318 reviewers are acknowledged for their constructive comments that have largely improved the
10
11 319 quality of this paper.

12
13
14 320 **References**

- 15
16 321 1. R. B. Georg, K. Newman, *J. Anal. At. Spectrom.*, 2015, 30, 1935-1944.
17
18 322 2. D. Foucher, H. Hintelmann, *Anal. Bioanal. Chem.*, 2006, 384: 1470-1478.
19
20 323 3. J. D. Blum, B.A. Bergquist, *Anal. Bioanal. Chem.*, 2007, 388, 353-359.
21
22 324 4. L. Yang, R.E. Sturgeon, *Anal. Bioanal. Chem.*, 2009, 393,377-385.
23
24 325 5. N. Estrade, J. Carignan, J.E. Sonke, et al., *Geostand. Geoanal. Res.*, 2010, 34, 79-93.
25
26 326 6. J. Masbou, D. Point, J.E. Sonke, *J. Anal. At. Spectrom.*, 2013, 28, 1620-1628.
27
28 327 7. R. S. Yin, X. B. Feng, D. Foucher, et al., *Chinese J. Anal. Chem.*, 2010, 38, 929-934.
29
30 328 8. A. Rua-Ibarz, E. Bolea-Fernandez, F. Vanhaecke, *Anal. Bioanal. Chem.*, 2016, 408,
31 329 417-429.
32
33 330 9. A. Berni, C. Baschieri, S. Covelli, et al., *Talanta*, 2016, 152, 179-187.
34
35 331 10. B.A. Bergquist, J.D. Blum, *Elements*, 2009, 5, 353-357.
36
37 332 11. J. D. Blum, L.S. Sherman, M.W. Johnson, *Annu. Rev. Earth Pl. Sc.*, 2014, 42, 249-269.
38
39 333 12. R. Yin, X. Feng, X. Li, et al., *TrEAC*, 2014, 2, 1-10.
40
41 334 13. K. Newman, *J. Anal. At. Spectrom.*, 2012, 27, 63-70.
42
43 335 14. W. Zheng, D. Obrist, D. Weis, et al., *Environ. Sci. Technol.* 2016, In review.
44
45 336 15. D. L. Pfeil, D. Stalvey, *American Laboratory* 2004, 36, 11-16.
46
47 337 16. R. Yin, X. Feng, B. Chen, et al., *Environ. Sci. Technol.* 2015, 49, 1347-1355.
48
49 338 17. H. Lin, D. Yuan, B. Lu, et al., *J. Anal. At. Spectrom.*, 2015, 30, 353-359.
50
51 339 18. W. I. Ridley, S. J. Stetson, *Applied Geochemistry*, 2006, 21, 1889-1899.
52
53 340 19. B. A. Bergquist, J. D. Blum, *Science* 2007, 318, 417-420.
54
55 341 20. A. Biswas, J.D. Blum, B.A. Bergquist, et al. *Environ. Sci. Technol.* 2008, 42, 8303-8309.
56
57 342 21. S.Y. Kwon, J.D. Blum, M.A. Chirby, et al., *Environ. Toxicol. Chem.*, 2013, 32,
58 343 2322-2330.
59
60

344 22. R. Yin, R. F. Lepak, D.P. Krabbenhoft, et al., Elementa: Science of the Anthropocene,
345 2016, 4, 000086.

1
2
3
4
5
6
7
8
9
10
11
12
13
14
15
16
17
18
19
20
21
22
23
24
25
26
27
28
29
30
31
32
33
34
35
36
37
38
39
40
41
42
43
44
45
46
47
48
49
50
51
52
53
54
55
56
57
58
59
60

1
2
3 346 **Figure captions**
4
5

6 347 **Figure 1** Hg gas phase separator for Hg isotope measurements in this study.

7 348 **Figure 2** Correlations between $^{205}\text{Tl}/^{203}\text{Tl}_{\text{measured}}$ and Tl concentrations (A), Hg
8 concentrations (B) and Hg/Tl ratios (C); Correlations between mass-bias correction factor (β)
9 and Tl concentrations (D), Hg concentrations (E) and Hg/Tl ratios (F).
10

11 351 **Figure 3** Correlation between ^{201}Hg and Tl (^{203}Tl : black circles; ^{205}Tl : blue circles) beam
12 intensities. Measurements were conducted by introducing 0.3 to 3.0 ng mL⁻¹ of Hg without
13 of Tl.
14
15
16
17
18

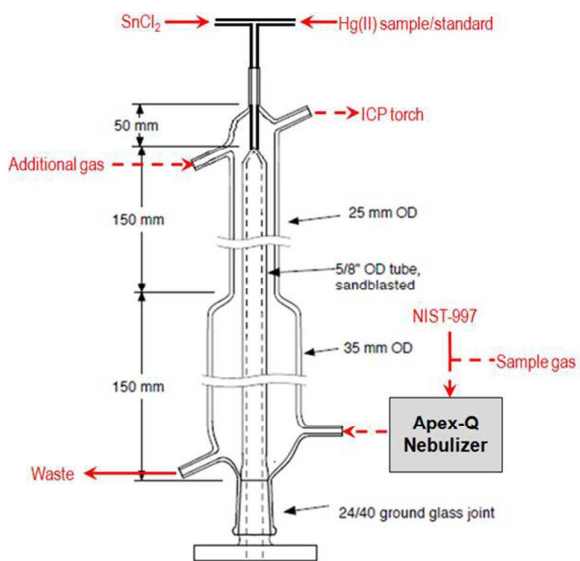
19 354 **Figure 4** Correlations between $^{\text{xxx}}\text{Hg}/^{198}\text{Hg}_{\text{true}}$ ratios and Hg concentrations over varied Tl
20 concentrations. Red circles represent UM-Almadén; blue circles represent NIST SRM 3133.
21

22 356 **Figure 5** Relationship between the standard error of $^{\text{xxx}}\text{Hg}/^{198}\text{Hg}_{\text{true}}$ ratios and Hg
23 concentration over varied Tl concentrations. Red circles represent UM-Almadén; blue
24 circles represent NIST SRM 3133.
25
26
27

28 359 **Figure 6** Variations of $^{205}\text{Tl}/^{203}\text{Tl}_{\text{measured}}$ (A), standard error of $^{205}\text{Tl}/^{203}\text{Tl}_{\text{measured}}$ (B), and
29 mass-bias correction factor β (C) over varied Tl concentrations. Dark circles represent that
30 measurements were based on NIST SRM 3133 of 0.5 ng mL⁻¹ Hg; tubular diamonds
31 represent that measurements were based on NIST-3133 of 1.0 ng mL⁻¹ Hg;
32
33
34

35 363 **Figure 7** Variations of $^{\text{xxx}}\text{Hg}/^{198}\text{Hg}_{\text{true}}$ ratios and standard errors (SE) over varied Tl
36 concentrations. Dark circles represent that measurements were based on NIST SRM 3133 of
37 0.5 ng mL⁻¹ Hg; tubular diamonds represent that measurements were based on NIST SRM
38 3133 of 1.0 ng mL⁻¹ Hg;
39
40
41
42

43 367 **Figure 8** Relationship of Hg isotopic compositions ($\delta^{202}\text{Hg}$, $\Delta^{199}\text{Hg}$ and $\Delta^{200}\text{Hg}$) to relative
44 Hg concentration differences between UM-Almadén and NIST SRM 3133 over varied Tl
45 concentrations. Row 2 is an expansion of row 1. Row 3 is a more detailed expansion of row
46 2. (Blue circles: 3 ng mL⁻¹ Tl; brown circles: 20 ng mL⁻¹ Tl; green circles: 30 ng mL⁻¹ Tl; red
47 circles: 50 ng mL⁻¹ Tl).
48
49
50
51
52
53
54
55
56
57
58
59
60

372 **Figure 1**

373

Figure 2

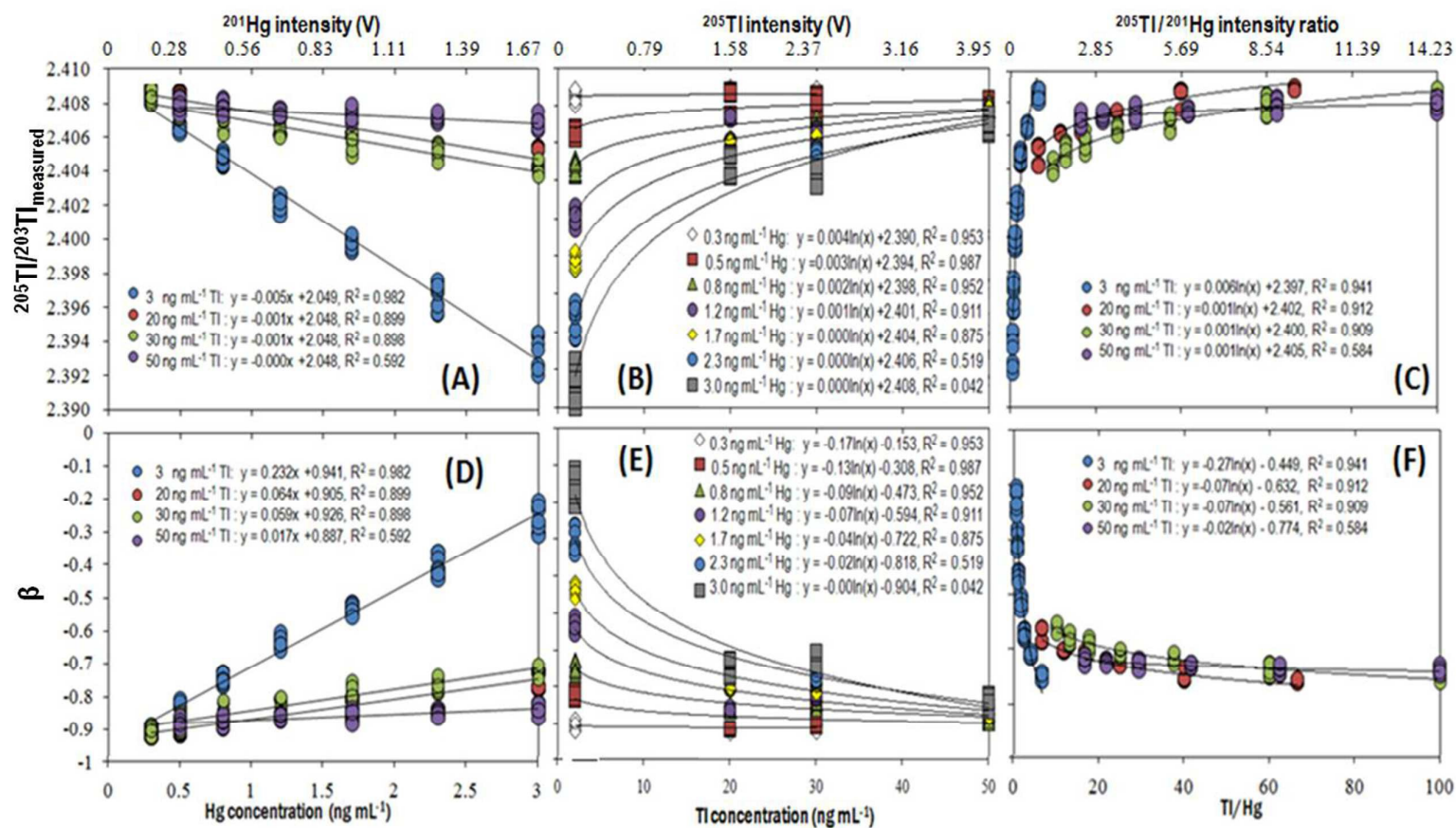


Figure 3

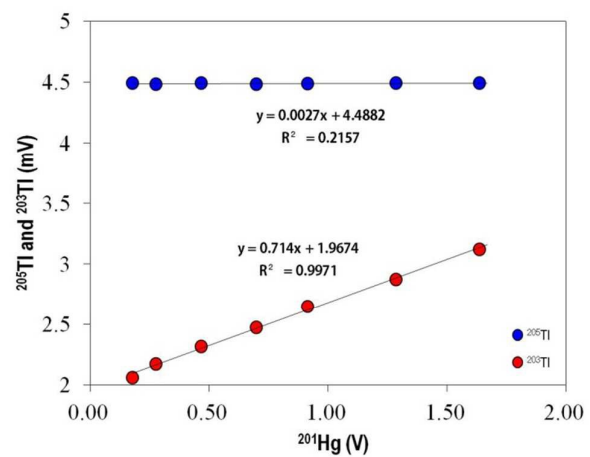


Figure 4

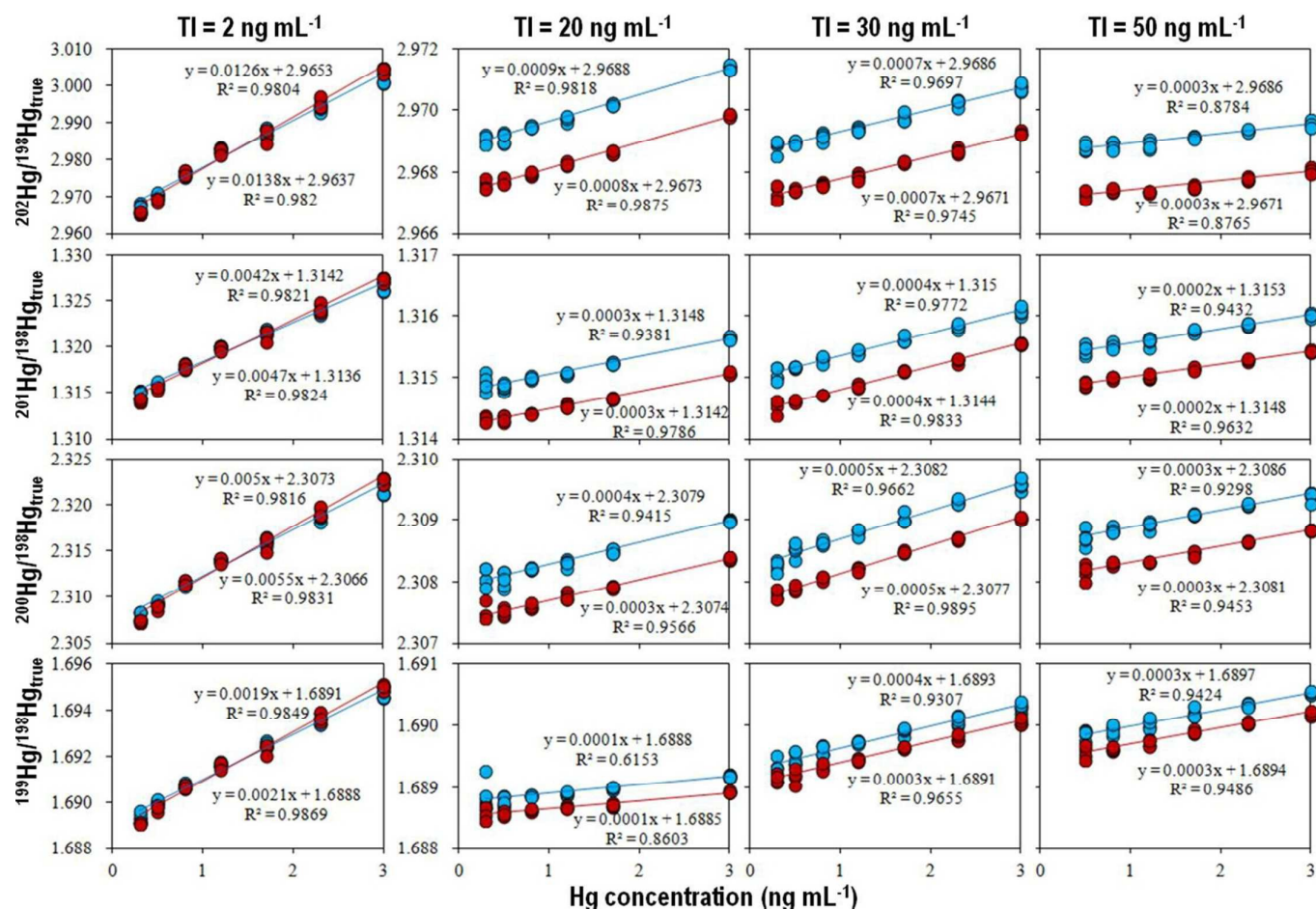


Figure 5

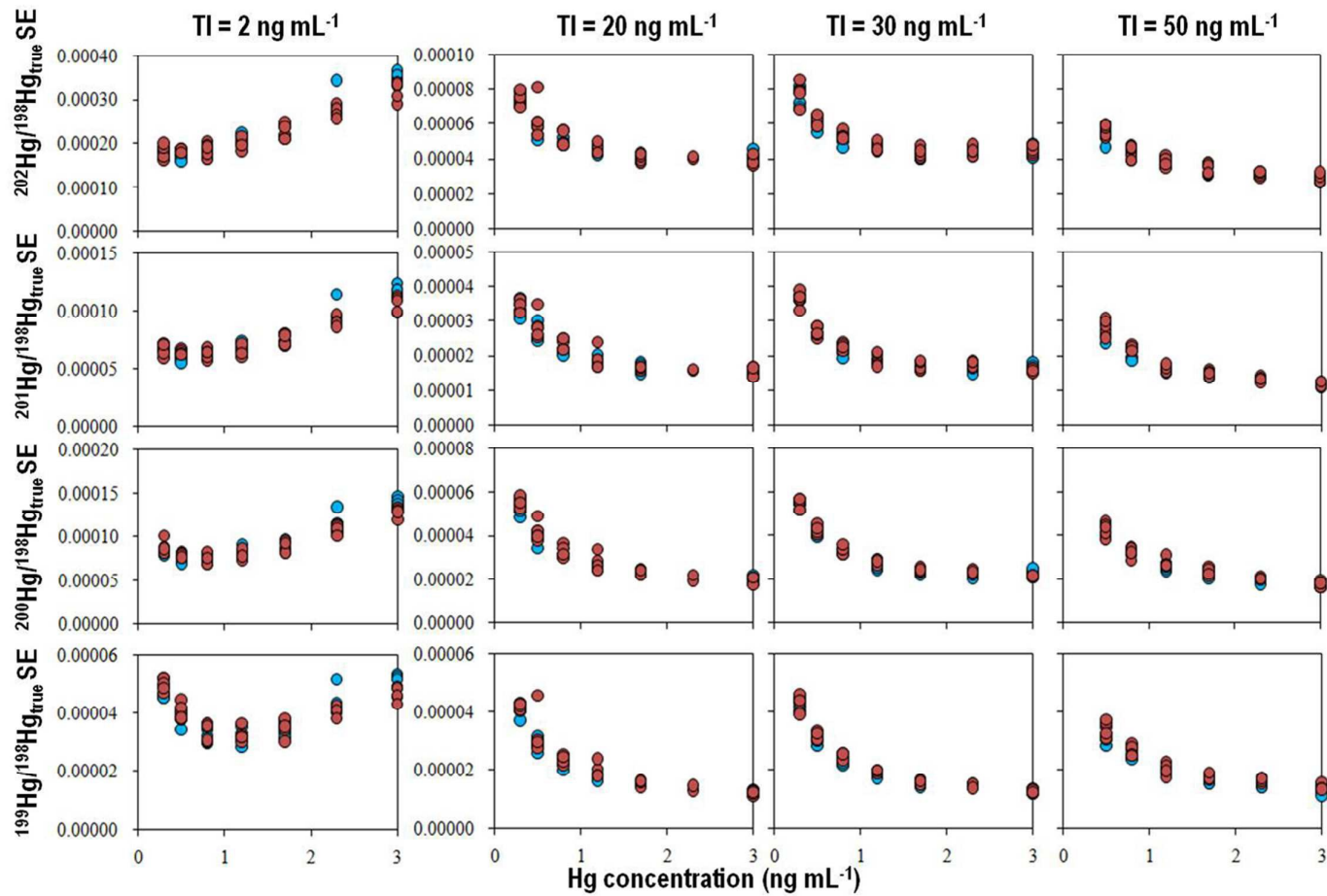


Figure 6

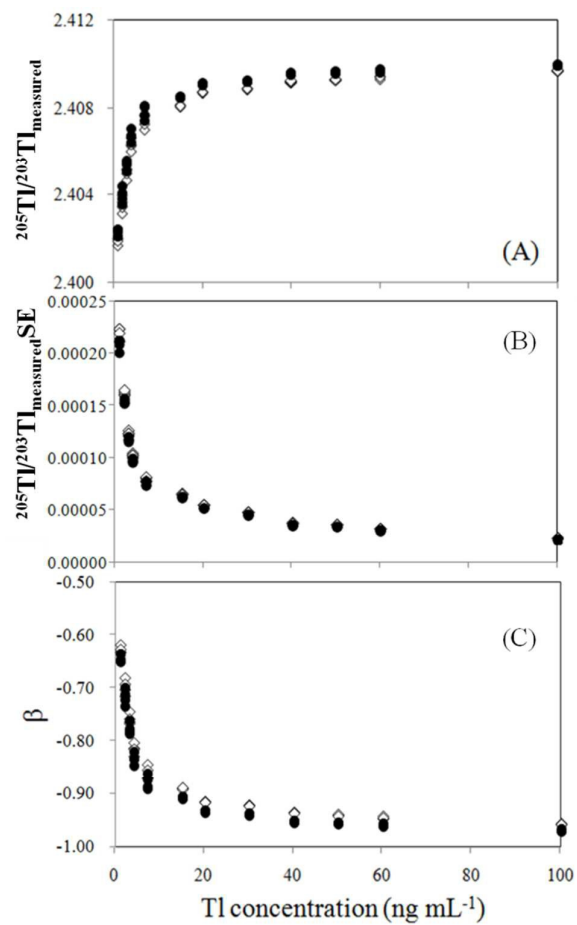


Figure 7

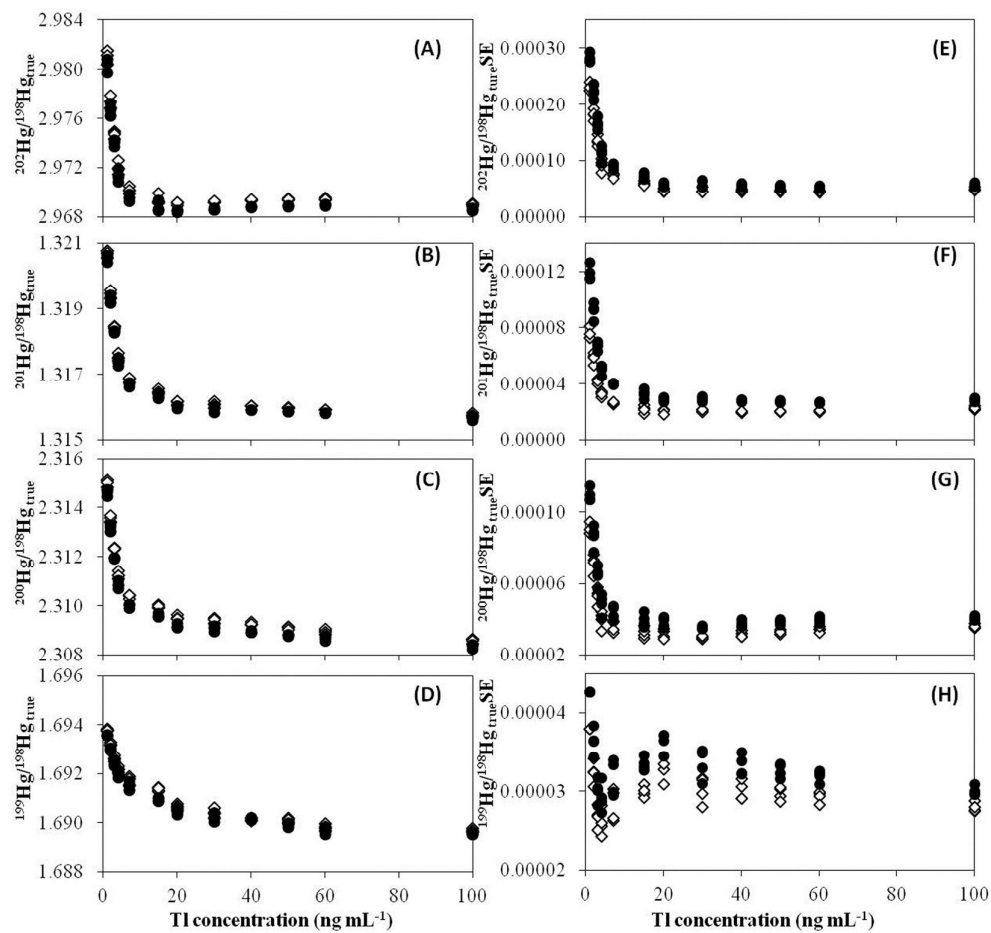
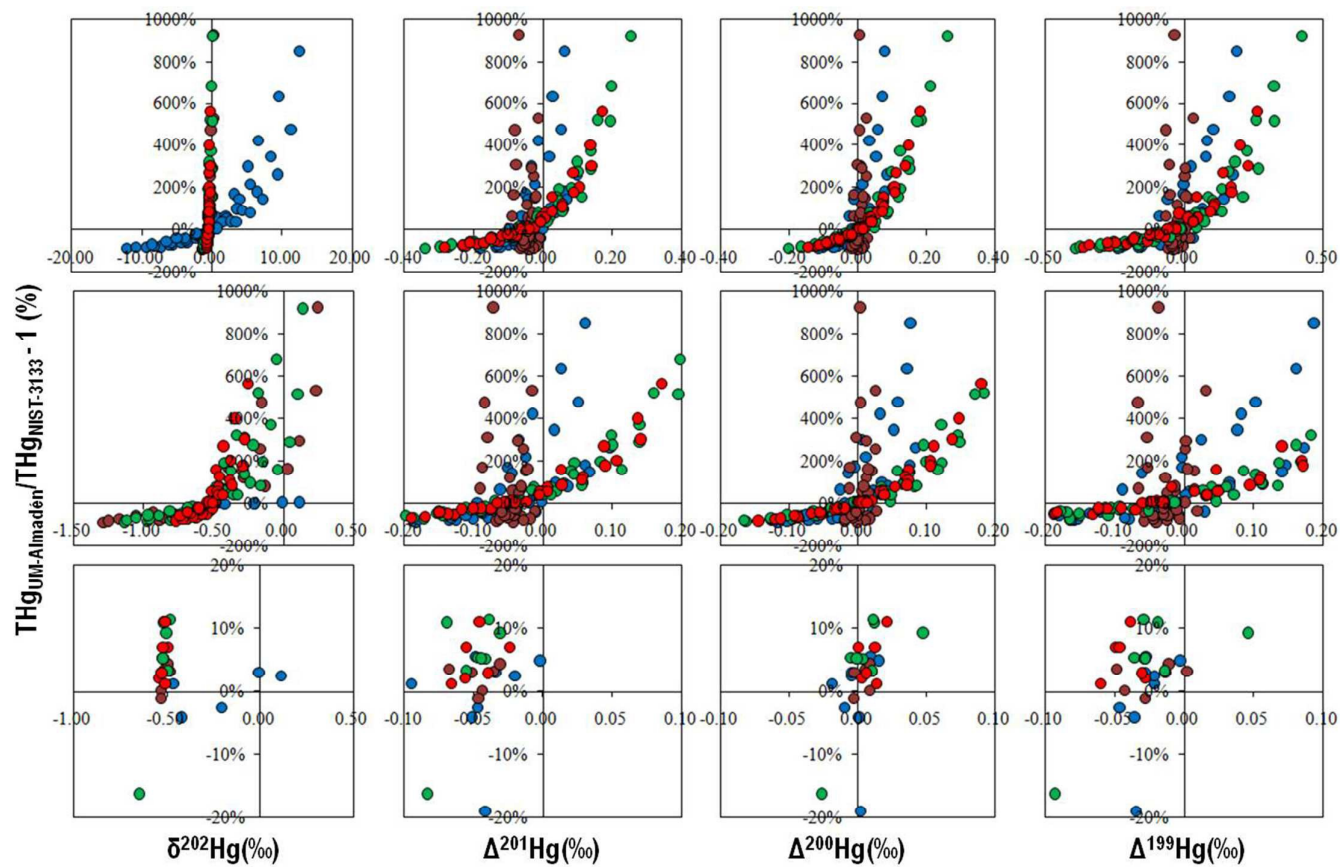


Figure 8



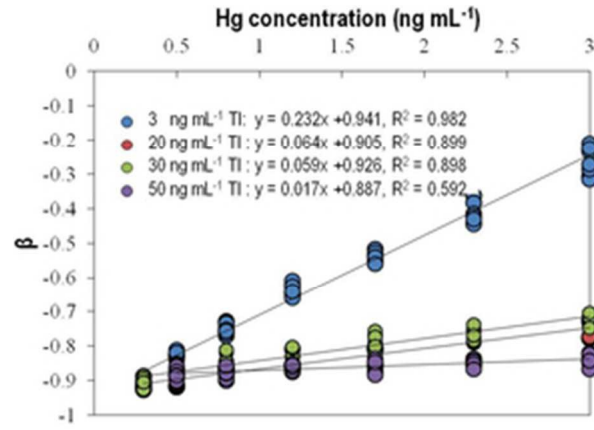
1
2
3
4
5
6
7
8
9
10
11
12
13
14
15
16
17
18
19
20
21
22
23
24
25
26
27
28
29
30
31
32
33
34
35
36
37
38
39
40
41
42
43
44
45
46
47
48
49

Table 1 Faraday cups configuration for Hg isotope ratio measurements

Cups isotopes	L4	L3	L2	L1	C	H1	H2	H3	H4
		¹⁹⁸ Hg	¹⁹⁹ Hg	²⁰⁰ Hg	²⁰¹ Hg	²⁰² Hg	²⁰³ Tl	²⁰⁵ Tl	

Table 2 Operating parameters during Hg isotope analysis

MC-ICP-MS Plasma parameters	
Sample gas	0.82–0.84 L min ⁻¹
Additional gas	0.23–0.25 L min ⁻¹
Cool gas	16.0 L min ⁻¹
Auxiliary gas	0.80 L min ⁻¹
RF power	1400 W
Apex-Q	
Heater temperature	100°C
Chiller temperature	2°C
Nebulizer	PFA-50
Tl solution uptake rate	0.05 mL min ⁻¹
Peristaltic pump	
Hg solution uptake rate	0.65 mL min ⁻¹



24x17mm (300 x 300 DPI)

1
2
3
4
5
6
7
8
9
10
11
12
13
14
15
16
17
18
19
20
21
22
23
24
25
26
27
28
29
30
31
32
33
34
35
36
37
38
39
40
41
42
43
44
45
46
47
48
49
50
51
52
53
54
55
56
57
58
59
60